Available online at www.sciencedirect.com
SCIENCE @ DIRECT®

Dyes and Pigments 71 (2006) 138–144

DYES and PIGMENTS
www.elsevier.com/locate/dyepig

# The enhancement effect of hydrogen bond on the third-order nonlinear optical properties

Shouchun Yin [a,b], Hongyao Xu [a,*], Wenfang Shi [b], Yachen Gao [c],
Yinlin Song [c], Ben Zhong Tang [a,d]

[a] *Faculty of Chemistry and Chemical Engineering, Anhui University, Key Laboratory of Environment-Friendly Polymer Materials of Anhui Province, Hefei 230039, China*
[b] *Department of Polymer Materials Science and Engineering, University of Science and Technology of China, Hefei 230026, China*
[c] *Department of Physics, Harbin Institute of Technology, Harbin 150001, China*
[d] *Department of Chemistry, The Hong Kong University of Science & Technology, Kowloon, Hong Kong, China*

Received 17 December 2004; received in revised form 11 March 2005; accepted 20 April 2005
Available online 18 August 2005

---

## Abstract

Three conjugated molecules', 4-phenylethynyl-4′-[*N*,*N*-diethylamino]azobenzene (**3a**), 4-phenylethynyl-4′-{[*N*-ethyl-*N*-(2-hydroxyethyl)]amino}azobenzene (**3b**), and 4-phenylethynyl-4′-[*N*,*N*-di(2-hydroxyethyl)amino]azobenzene (**3c**), nonlinear optical properties were determined using Z-scan technique with 532 nm, 8 ns laser pulses. The results indicate that these compounds possess large nonlinear optical absorptions, which are attributed to the long π-conjugation structure owing to the substituent of phenylethynyl group. The nonlinearity increases with an increase in the number of hydroxyl group, due to the regular arrangement induced by the strong hydrogen bond interaction between hydroxyl groups of molecules. Their nonlinearity enhancement mechanism was studied by FT-IR spectroscopy.

*Keywords:* Nonlinear optical; Azo dyes; Z-scan; Hydrogen bond; Synthesis; Chromophore

---

## 1. Introduction

Conjugated organic nonlinear optical (NLO) materials are drawing steady attention because of their wide applications in various fields such as optical communication, optical data storage, optical information processing, and optical limiting [1]. During the past two decades, many organic materials such as azobenzene, porphyrins, phthalocyanines, polydiacetylenes and polyacetylenes have been synthesized [2–10].

To enhance the application viability of the conjugated organic NLO materials in optoelectronic and photonic devices, a collective effort from physicists, chemists and material scientists is currently in progress to understand the fundamental relationship between optical response and molecular structure. Schuling found that the third-order nonlinear optical susceptibility ($\gamma$) of a molecule depends on $\gamma_e^0$, a term related to the movement of electron, and $\beta$, the second-order nonlinear optical susceptibility of the molecule [11]. Rustagi and Ducuing discovered that in π-conjugated organic compounds, electrons could move in large molecular orbitals that result from the linear superposition of the carbon $P_z$ atomic orbitals, leading to very high $\chi^{(3)}$ [12]. The third-order nonlinear optical susceptibility increases with the conjugation length of a molecule. It is widely accepted that $\chi^{(3)}$ changes with energy gap between the highest occupied (HOMO) and the lowest unoccupied (LUMO)

---

[*] Corresponding author. Fax: +86 551 5108203.
*E-mail address:* hongyaoxu@163.com (H. Xu).

0143-7208/$ - see front matter © 2005 Elsevier Ltd. All rights reserved.
doi:10.1016/j.dyepig.2005.04.019

molecular orbitals. Specifically, theoretical considerations predict for one-dimensional conjugated systems with extended π-electron delocalization [13]: $\chi^{(3)} \propto E_g^{-n}$ and Prasad presented $n = 6$, which is drawn from the study of one-dimensional conjugated polydiacetylene systems [14]. Many chemists and material scientists have utilized the hydrogen bond to give the bigger third-order nonlinear optical materials [15–19]. However, the effective degree of hydrogen bond on the NLO properties, to our knowledge, has not been investigated.

In this work, we investigated three long conjugated substituted azobenzenes containing phenylethynyl group, namely, 4-phenylethynyl-4′-[*N*,*N*-diethylamino]azobenzene, 4-phenylethynyl-4′-{[*N*-ethyl-*N*-(2-hydroxyethyl)]-amino}azobenzene, 4-phenylethynyl-4′-[*N*,*N*-di(2-hydroxyethyl)amino]azobenzene (Scheme 1) that differ only in the number of hydroxyl groups in order to investigate the effect of hydrogen bond on the NLO properties.

## 2. Experimental

### 2.1. Materials and measurements

Phenylacetylene was purchased from Fluka and distilled from calcium hydride under reduced pressure before use. $PdCl_2(PPh_3)_2$, *N*-ethylaniline, *N*,*N*-diethylaniline and 4-bromoaniline were purchased from Aldrich. FT-IR spectra were recorded as KBr pellets on a Nicolet 170SX Spectrometer. $^1H$ and $^{13}C$ NMR spectra were collected on an AVANCE/DMX-500 MHz Bruker NMR Spectrometer. UV–vis spectra were recorded on a Shimadzu UV-265 Spectrometer using a 1-cm square quartz cell. Elementary analyses were conducted on Elementar Vario EL-III elementary analysis apparatus. Melting points (mp) were measured on a Yanaco micro melting point apparatus.

The third-order nonlinear optical properties were investigated using the Z-scan technique [20]. In our experiment, a THF solution of the compound was placed in a 2-mm quartz cell. The optical response of the sample was measured with a Q-switched ns/ps Nd:YAG laser system continuum ($\lambda = 532$ nm, pulse width $\tau = 8$ ns). The relation between the normalized transmittance $T(z)$ and $z$ position was obtained by moving the samples along the axis of the incident beam ($z$ direction) with respect to the focal point. The incident and transmitted energies were detected simultaneously by an energy meter (Laser Precision Corporation Rjp-735). The input energy was 180 μJ.

### 2.2. Synthesis

#### 2.2.1. N-Ethyl-N-(2-hydroxylethyl)aniline (**1b**)

A mixture of 15 mL (0.225 mol) of 2-chloroethanol, 19 mL (0.15 mol) of *N*-ethylaniline, 50 mL of distilled water and 15 g (0.15 mol) of $CaCO_3$ was refluxed for 20 h. The mixture was then filtered and the filtrate was saturated with NaCl and extracted with acetic ether. The organic layer was dried with anhydrous magnesium sulfate and concentrated. The crude product was distilled under reduced pressure to give a pale yellow viscous oil (122–124 °C/2 mmHg). Yield: 67% (16.6 g). $^1H$ NMR (500 MHz, $CDCl_3$), $\delta$ (ppm): 1.15 (3H, t, $J = 7.1$ Hz, $CH_2CH_3$), 1.78 (1H, s, $OH$), 3.41 (2H, q, $CH_2CH_3$), 3.46 (2H, t, $J = 5.5$ Hz, $CH_2CH_2OH$), 3.78 (2H, t, $CH_2CH_2OH$), 6.72 (1H, dd, $J = 7.1$ Hz, 4-H), 6.78 (2H, d, $J = 7.8$ Hz, 2- and 6-H), 7.23 (2H, dd, 3- and 5-H). FT-IR (KBr), $\nu$ ($cm^{-1}$): 3341 (–OH), 2969 ($-CH_3$), 2873 ($-CH_2$), 1597 (–Ar).

#### 2.2.2. N,N-Di(2-hydroxyethyl)aniline (**1c**)

This was prepared as above from aniline. The crude product was distilled under reduced pressure to give

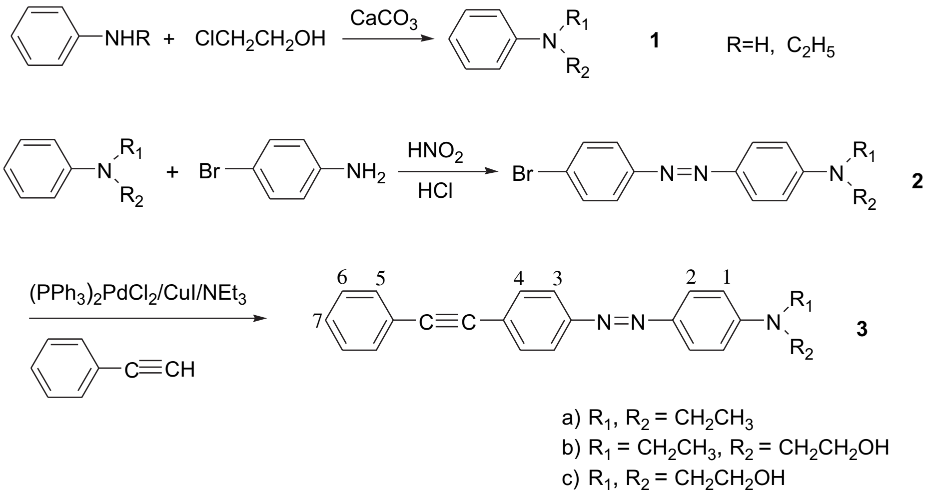

Scheme 1. Synthetic route and serial number of hydrogen atom of benzene ring in **2** and **3**.

a pale yellow viscous oil (178–184 °C/2 mmHg). Yield: 55%. $^1$H NMR (500 MHz, DMSO), $\delta$ (ppm): 3.39 (4H, t, $J = 5.4$ Hz, C$H_2$CH$_2$OH), 3.52 (4H, t, CH$_2$C$H_2$OH), 4.72 (2H, s, O$H$), 6.53 (1H, dd, $J = 7.2$ Hz, 4-H), 6.66 (2H, d, $J = 8.2$ Hz, 2- and 6-H), 7.12 (2H, dd, 3- and 5-H). FT-IR (KBr), $\nu$ (cm$^{-1}$): 3328 (–OH), 2945, 2882 (–CH$_2$), 1597 (–Ar).

### 2.2.3. *4-Bromo-4′-[(N,N-diethyl)amino]-azobenzene (**2a**)*

4-Bromoaniline (3.5 g, 20 mmol) was dissolved in an ice–water solution of sodium nitrite (1.36 g, 20 mmol). After cooling to 0 °C, the solution was added to conc. hydrochloric acid (8 mL) and stirred for 30 min. Then the mixture was added dropwise to 400 mL aqueous buffer solution of acetic acid–sodium acetate (pH $\approx$ 6) containing 3.7 g *N*,*N*-diethylaniline (21 mmol) and stirred for 2 h at 0–5 °C. The resulting precipitate was filtered and rinsed with water twice. The crude product was recrystallized from ethanol–petroleum ether twice to give yellow crystals with 85% yield (5.6 g). $^1$H NMR (500 MHz, CDCl$_3$), $\delta$ (ppm): 1.24 (6H, t, $J = 7.1$ Hz, CH$_2$C$H_3$), 3.46 (4H, q, C$H_2$CH$_3$), 6.73 (2H, d, $J = 7.7$ Hz, 1-H), 7.58 (2H, d, $J = 8.5$ Hz, 4-H), 7.71 (2H, d, 3-H), 7.85 (2H, d, 2-H) (the serial number of hydrogen atom of benzene ring is given in Scheme 1). FT-IR (KBr), $\nu$ (cm$^{-1}$): 2974 (–CH$_3$), 2945, 2882 (–CH$_2$), 1595 (–Ar).

### 2.2.4. *4-Bromo-4′-[N-ethyl-N-(2-hydroxyethyl)amino]-azobenzene (**2b**)*

This was prepared as above from *N*-ethyl-*N*-(2-hydroxyethyl)aniline. The product was yellow crystal. Yield: 81%. $^1$H NMR (500 MHz, CDCl$_3$), $\delta$ (ppm): 1.24 (3H, t, $J = 7.1$ Hz, CH$_2$C$H_3$), 1.63 (1H, s, O$H$), 3.54 (2H, q, C$H_2$CH$_3$), 3.59 (2H, t, $J = 5.5$ Hz, C$H_2$CH$_2$OH), 3.87 (2H, t, CH$_2$C$H_2$OH), 6.81 (2H, d, $J = 8.8$ Hz, 1-H), 7.59 (2H, d, $J = 8.6$ Hz, 4-H), 7.71 (2H, d, 3-H), 7.85 (2H, d, 2-H). FT-IR (KBr), $\nu$ (cm$^{-1}$): 3346 (–OH), 2949 (–CH$_3$), 2882 (–CH$_2$), 1598 (–Ar).

### 2.2.5. *4-Bromo-4′-[(N,N-dihydroxyethyl)amino]-azobenzene (**2c**)*

This was prepared as above from *N*,*N*-di-(2-hydroxyethyl)aniline. The product was yellow piece crystal. Yield: 83%. $^1$H NMR (500 MHz, DMSO), $\delta$ (ppm): 3.55 (4H, t, $J = 5.5$ Hz, C$H_2$CH$_2$OH), 3.60 (4H, t, CH$_2$C$H_2$OH), 4.84 (1H, s, O$H$), 6.86 (2H, d, $J = 9.1$ Hz, 1-H), 7.70 (2H, d, $J = 8.9$ Hz, 4-H), 7.76 (2H, d, 3-H), 7.85 (2H, d, 2-H). FT-IR (KBr), $\nu$ (cm$^{-1}$): 3280 (–OH), 2945, 2882 (–CH$_2$), 1597 (–Ar).

### 2.2.6. *4-Phenylethynyl-4′-[N,N-di(2-ethylamino)]-azobenzene (**3a**)*

Under nitrogen, 49 mg (0.07 mmol) PdCl$_2$(PPh$_3$)$_2$, 7 mg (0.036 mmol) CuI and 2.4 g (7 mmol) 4-bromo-4′-[*N*,*N*-(diethyl)amino]azobenzene were dissolved in 10 mL Et$_3$N and 25 mL THF. To this solution 0.86 mL (8.4 mmol) phenylacetylene was added and the resultant mixture was refluxed for 3 h. After cooling to room temperature, the precipitate in the mixture was filtered. The filtrate was concentrated and redissolved in THF and the THF solution was added dropwise into ethanol under stirring. The dissolution–precipitation process was repeated three times and the finally isolated precipitant was filtered to give 2.2 g red solid (yield 90%). $T_m = 190$–192 °C. Elem. Anal. Calcd for $C_{18}H_{19}N_3$: C, 81.59; H, 6.52; N, 11.90. Found: C, 81.29; H, 6.53; N, 12.18. $^1$H NMR (500 MHz, CDCl$_3$), $\delta$ (ppm): 1.25 (6H, t, $J = 7.0$ Hz, CH$_2$C$H_3$), 3.47 (4H, q, C$H_2$CH$_3$), 6.73 (2H, d, $J = 8.3$ Hz, 1-H), 7.36 (1H, dd, $J = 5.2$ Hz, 7-H), 7.37 (2H, t, $J = 6.7$ Hz, 6-H), 7.55 (2H, d, 5-H), 7.62 (2H, d, $J = 8.1$ Hz, 4-H), 7.83 (2H, d, 3-H), 7.87 (2H, d, 2-H) (the serial number of hydrogen atom of benzene ring is given in Scheme 1). $^{13}$C NMR (125 MHz, CDCl$_3$), $\delta$ (ppm): 13.5 (CH$_2$$C$H$_3$), 45.5 ($C$H$_2$CH$_3$), 90.5, 91.8 (C$\equiv$C), 111.8, 123.0, 124.1, 124.6, 126.3, 129.1, 132.4, 132.8, 133.1, 144.0, 151.2, 153.5 (Ph). FT-IR (KBr), $\nu$ (cm$^{-1}$): 2973 (–CH$_3$), 2892 (–CH$_2$), 1598 (–Ar).

### 2.2.7. *4-Phenylethynyl-4′-{[N-ethyl-N-(2-hydroxyethyl)]amino}azobenzene (**3b**)*

This was prepared as above from 4-bromo-4′-{[*N*-ethyl-*N*-(2-hydroxyethyl)]amino}azobenzene. The crude product was recrystallized from ethanol–petroleum ether twice to give deep-red crystals with 86% yield. $T_m = 221$–223 °C. Elem. Anal. Calcd for $C_{18}H_{19}N_3$: C, 78.05; H, 6.23; N, 11.38. Found: C, 77.52; H, 6.18; N, 11.32. $^1$H NMR (500 MHz, DMSO), $\delta$ (ppm): 1.15 (3H, t, $J = 7.0$ Hz, CH$_2$C$H_3$), 3.50 (2H, q, C$H_2$CH$_3$), 3.52 (2H, t, $J = 5.7$ Hz, C$H_2$CH$_2$OH), 3.61 (2H, t, CH$_2$C$H_2$OH), 4.82 (1H, s, O$H$), 6.85 (2H, d, $J = 8.8$ Hz, 1-H), 7.44 (1H, dd, $J = 5.2$ Hz, 7-H), 7.45 (2H, t, $J = 5.3$ Hz, 6-H), 7.59 (2H, d, 5-H), 7.68 (2H, d, $J = 8.2$ Hz, 4-H), 7.77 (2H, d, 3-H), 7.79 (2H, d, 2-H). $^{13}$C NMR (125 MHz, DMSO), $\delta$ (ppm): 12.0 (CH$_2$$C$H$_3$), 45.1 ($C$H$_2$CH$_3$), 52.1 ($C$H$_2$CH$_2$OH), 58.3 (CH$_2$$C$H$_2$OH), 89.3, 91.1 (C$\equiv$C), 111.2, 122.2, 122.8, 125.3, 128.8, 131.4, 132.4, 142.3, 150.9, 152.0 (Ph). FT-IR (KBr), $\nu$ (cm$^{-1}$): 3580, 3420 (–OH), 2975 (–CH$_3$), 2919 (–CH$_2$), 1598 (–Ar).

### 2.2.8. *4-Phenylethynyl-4′-[N,N-di(2-hydroxyethyl)-amino]azobenzene (**3c**)*

This was prepared as above from 4-bromo-4′-[(*N*,*N*-di(2-hydroxyethyl)amino)azobenzene. The crude product was recrystallized from ethanol–petroleum ether twice to give brown-red crystals with 83% yield. $T_m = 235$–237 °C. Elem. Anal. Calcd for $C_{18}H_{19}N_3$: C, 74.81; H, 5.97; N, 10.91. Found: C, 74.58; H, 6.03; N, 10.51. $^1$H NMR (500 MHz, DMSO), $\delta$ (ppm): 3.57 (2H, $J = 5.7$ Hz, t, C$H_2$CH$_2$OH), 3.60 (2H, t,

$CH_2CH_2OH$), 4.85 (1H, s, O*H*), 6.87 (2H, d, $J = 8.7$ Hz, 1-H), 7.44 (1H, dd, $J = 5.7$ Hz, 7-H), 7.45 (2H, t, $J = 5.5$ Hz, 6-H), 7.59 (2H, d, 5-H), 7.68 (2H, d, $J = 8.4$ Hz, 4-H), 7.77 (2H, d, 3-H), 7.79 (2H, d, 2-H). $^{13}C$ NMR (125 MHz, DMSO), $\delta$ (ppm): 53.0 ($CH_2CH_2OH$), 58.0 ($CH_2CH_2OH$), 89.2, 91.2 ($C{\equiv}C$), 111.4, 121.9, 122.1, 122.9, 125.2, 128.8, 129.0, 131.3, 132.4, 142.3, 151.2, 151.9 (Ph). FT-IR (KBr), $\nu$ ($cm^{-1}$): 3410, 3220 (–OH), 2949 (–$CH_3$), 2874 (–$CH_2$), 1598 (–Ar).

## 3. Results and discussion

### 3.1. Synthesis

The synthetic route of the compounds is shown in Scheme 1. The diazotization-coupling reaction of 4-bromoaniline with aniline derivative **1** was made in the buffer solution of acetic acid and sodium acetate (pH ≈ 6) in order to keep the diazo salt in high concentration. Compound **3** was obtained in high yield using $PdCl_2(PPh_3)_2$/CuI as catalysts under refluxing in our work instead of room temperature reported in other pertinent papers, because of the bigger stereo bulkiness of benzene ring in the phenylacetylene and inertial aryl halides reagent [21].

### 3.2. Electronic spectra

Fig. 1 shows the linear UV–vis absorption spectra of **3a–c** at 20 °C in THF solutions measured on a Shimadzu UV-265 Spectrometer. The absorption spectra exhibit maximum peaks at 454, 381 and 308 nm for **3a**, 458, 385 and 310 nm for **3b**, and 464, 387 and 313 nm for **3c**. While the azobenzene without phenylethynyl group shows absorption peaks at 255 and 360 nm, the absorption peaks of **3a–c** significantly shift to longer wavelengths, which should be attributed to the longer π-conjugations in the molecules of **3a–c** [22]. When the substituent changes from $C_2H_5$ to $C_2H_4OH$, the absorption peaks' red shift to longer wavelengths, such as 454, 381, 308 nm for **3a** to 458, 385, 310 nm for **3b**. With the number of $C_2H_4OH$ group increasing, the absorption maximum further shifts toward longer wavelengths: 458, 385, 310 nm for **3b** to 464, 387, 313 for **3c**. This may be explained by *J*-type aggregation and regular arrangement of azobenzene molecules due to strong interactions of hydroxyl group in the substituents through hydrogen bond formation [23]. The similar phenomena were observed in the system of Wu et al. [23].

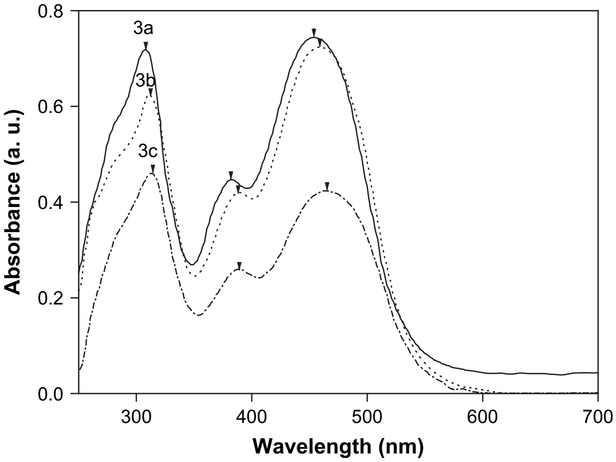

Fig. 1. UV–vis spectra of THF solutions of **3a–c**.

### 3.3. Nonlinear optical properties

The nonlinear absorption coefficients of these compounds were measured by Z-scan technique. In our experiment, the samples were moved along the direction of laser beam around the focus ($z = 0$) forward or backward. The transmittance was simultaneously recorded by a power meter with and without an aperture in the far field of lens as the function of sample position. The result of Z-scan with aperture confirmed that nonlinear refraction didn't contribute to the third-order nonlinear response. Thus, the $\chi^{(3)}$ measured in this experiment was totally attributed to nonlinear absorption of molecules ($\alpha_2$). Fig. 2 shows the open aperture Z-scan transmittance for **3a–c** measured by using a Q-switched ns/ps Nd:YAG laser system continuum with 8 ns pulse width at a wavelength of 532 nm. As can be seen from Fig. 2, a deep valley at the focus ($z = 0$) unambiguously indicates the intensity-dependent absorption.

In theory, the normalized transmittance for the open aperture can be written as [20,24]

$$T(z,s=1)=\sum_{m=0}^{\infty}\frac{[-q_0(z)]^m}{(m+1)^{3/2}},\ \text{for } |q_0|<1 \tag{1}$$

where $q_0(z)=\alpha_2 I_0(t)L_{\text{eff}}/\left(1+z^2/z_0^2\right)$, $\alpha_2$ is the nonlinear absorption coefficient, $I_0(t)$ is the intensity of laser beam at focus ($z = 0$), $L_{\text{eff}}=[1-\exp(-\alpha_0 L)]/\alpha_0$ is the effective thickness with $\alpha_0$ being the linear absorption coefficient and $L$ the sample thickness, $z_0$ is the diffraction length of the beam, and $z$ is the sample position. The solid curves for **3a–c** in Fig. 2 are fitted by using Eq. (1) with the parameters in our experiment and the nonlinear absorption coefficient $\alpha_2 = 2.0 \times 10^{-10}$, $2.4 \times 10^{-10}$ and $2.6 \times 10^{-10}$ (m/W) for **3a**, **3b**, and **3c**, respectively. The $\chi^{(3)}$ can be calculated from the following equation:

$$\chi^{(3)}(\text{esu})=9\times10^{8}\,\frac{\varepsilon_0 n_0^2 c^2 \alpha_2}{4\pi\omega} \tag{2}$$

where $\varepsilon_0$ is the permittivity of vacuum, $c$ the speed of light, and $n_0$ the refractive index of the medium and

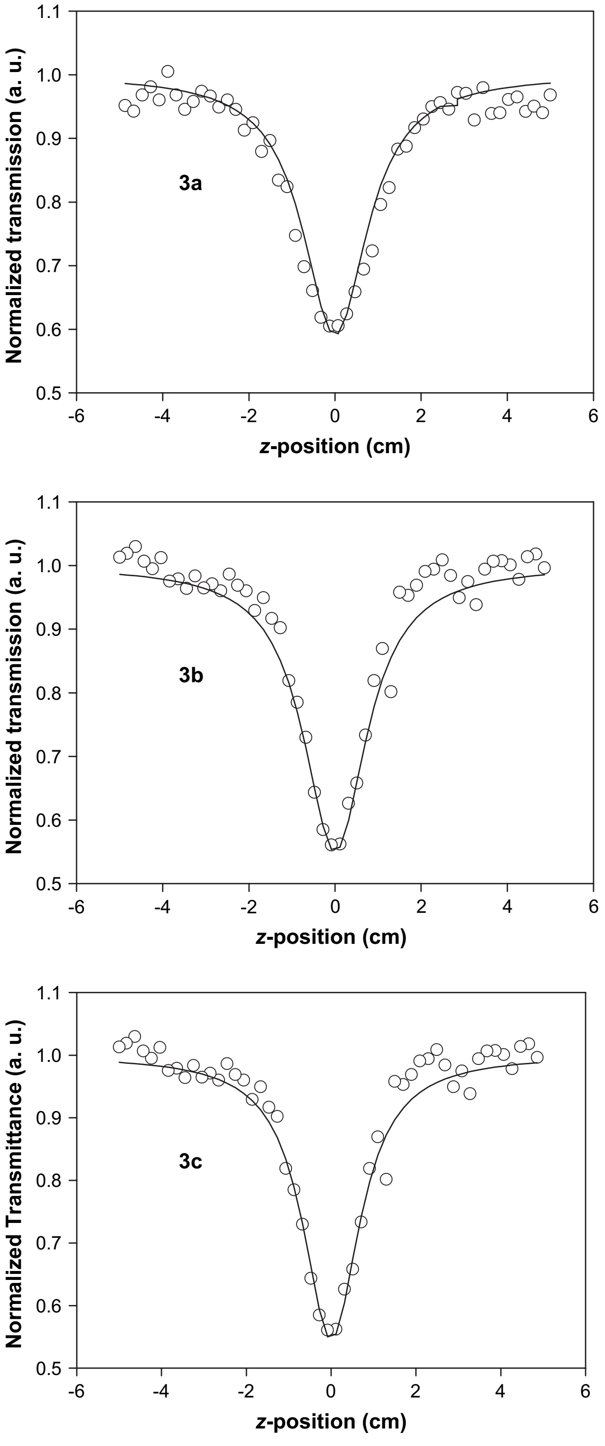

Fig. 2. Z-scan data of open aperture measured showing a strong nonlinear absorption near the lens focus: (circles) experimental data; (solid line) theoretical curve. The theoretical curve is fitted by using Eq. (1) with the nonlinear absorption coefficient $\alpha_2$.

$\omega = 2\pi c/\lambda$. Thus, the nonlinear susceptibilities are $6.5 \times 10^{-12}$, $7.0 \times 10^{-12}$ and $7.3 \times 10^{-12}$ esu for **3a**, **3b**, and **3c**, respectively. These nonlinear absorption coefficients are larger than that of [4-(4′-cyanoazophenylyl)oxy]-1-hexanol reported by Xu et al. [25]. The large nonlinear absorption coefficient can be attributed to the longer π-conjugation of **3a**–**c**, which is consistent with the results observed in the UV–vis spectra. The Im$\chi^{(3)}$ value increases with the increasing number of hydroxyethyl groups ($CH_2CH_2OH$) in the molecules. This may be attributed to more effective π-conjugation in the compounds **3c** and **3b** due to the aggregation and regular arrangement of molecules induced by the strong interaction between the hydroxyethyl groups in different molecules. This result further confirms the formation of hydrogen bonds between different molecules with hydroxyl groups. Similar phenomenon has been observed by Liang et al. [26].

### *3.4. Enhancement mechanism of Im$\chi^{(3)}$*

FT-IR spectroscopy is a suitable technique for investigating particular intermolecular interactions [27,28]. FT-IR absorption changes, in terms of strength and positions of characteristic functional groups, are attributable to the existence of specific intermolecular and/or intramolecular interactions. Therefore, we use FT-IR spectra of these compounds to elucidate the enhancement effect of hydrogen bond on the nonlinear optical susceptibility.

Whereas **3a** has no absorption in the region of 3000–3800 cm$^{-1}$, **3b** and **3c** have strong characteristic absorption band in the same spectral region, attributed to the hydroxyl vibrations. Therefore, any change in the FT-IR spectra in this region is attributed to the change in the chemical environments of the hydroxyl groups, especially the formation of hydrogen bonds. Hydrogen bonds may be cleaved or weakened by heating [29,30]. Figs. 3 and 4 show the expanded infrared spectra in the region of 3000–3800 cm$^{-1}$ at 20 and 60 °C for **3b** and **3c**, respectively. From Fig. 3, it can be seen that the free O–H stretching vibration

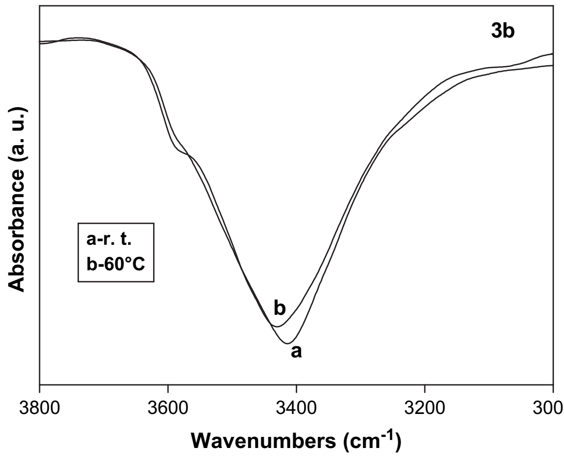

Fig. 3. Expanded FT-IR spectra recorded in the region of 3800–3000 cm$^{-1}$ for **3b** at 20 and at 60 °C.

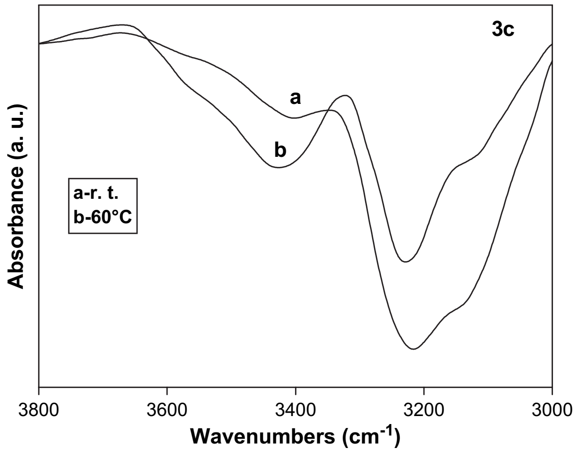

Fig. 4. Expanded FT-IR spectra recorded in the region of 3800–3000 $cm^{-1}$ for **3c** at 20 and at 60 °C.

peak located at 3580 $cm^{-1}$ does not shift. However, its strength is significantly enhanced and the peak area increased when the sample is heated from 20 to 60 °C. The broad strong characteristic absorption band at 3420 $cm^{-1}$, which may be assigned to the dimeric species (Fig. 5a) resulted from hydrogen bond interaction between the two molecules of **3b**, shifts toward higher wavenumber from 3420 to 3428 $cm^{-1}$. Its intensity is, however, weakened and the absorption peak area decreases, indicating that the hydrogen bond interaction between molecules of **3b** at 60 °C is weaker than that at 20 °C [31].

The similar phenomena are also observed in the infrared spectra of **3c** (Fig. 4). However, different from that of **3b**, a new stronger vibration absorption band with a peak at 3220 $cm^{-1}$ besides very weak free O–H stretching band at 3580 $cm^{-1}$ and a broad vibration peak at 3410 $cm^{-1}$ exists in the spectrum of **3c**. The vibration absorption peak at 3410 $cm^{-1}$ may be assigned to the dimeric species (Fig. 5b) resulting from hydrogen bond interaction between the two molecules of **3c**, whereas the stronger vibration band with an absorption peak at 3220 $cm^{-1}$ may be attributed to the formation of "polymeric" species (Fig. 5c) from hydrogen bond interaction among different molecules of **3c** [31]. The

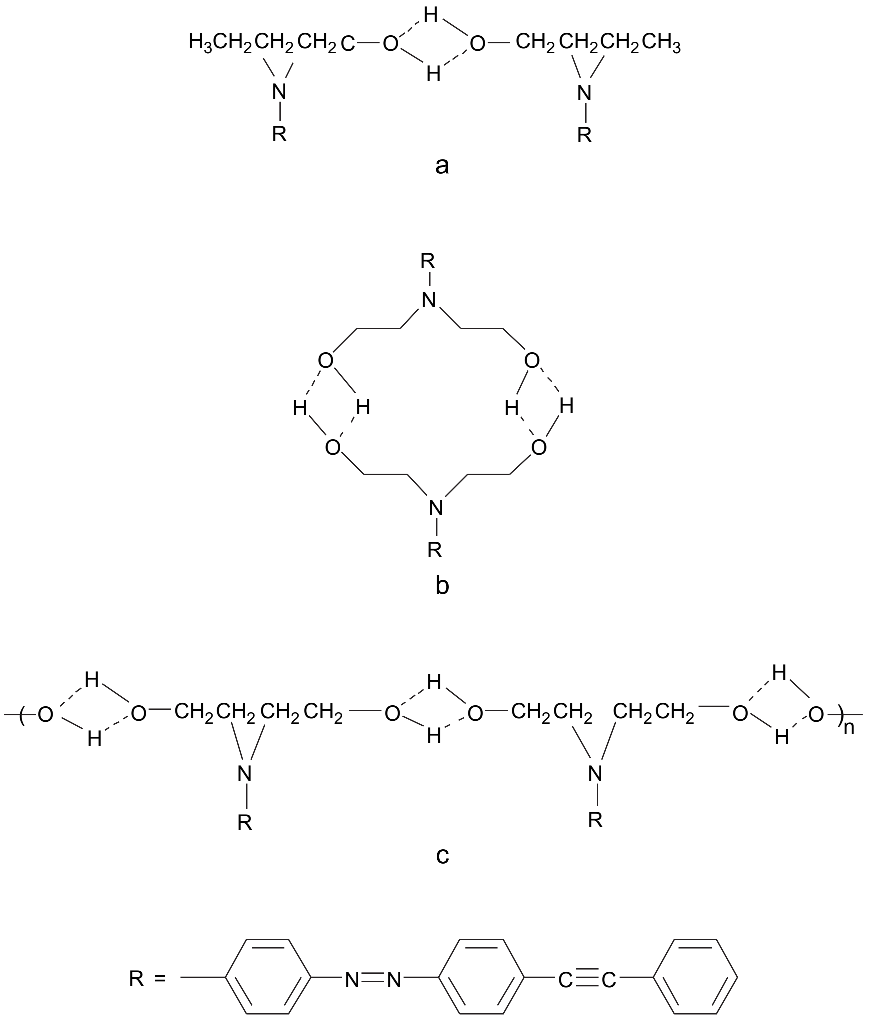

Fig. 5. Proposed hydrogen bond interactions in **3b** and **3c**.

similar phenomena were also confirmed in the work of Finch and Lippincott [29].

The stronger "polymeric" hydrogen bond (Fig. 5c) is the dominant existence pattern in **3c** and its absorption intensity is significantly weakened when heated to 60 °C. Compared with that in **3b**, the broad absorption band at 3410 $\mathrm{cm}^{-1}$ in **3c** associated with the hydrogen bond absorption of the dimeric species is contrarily enhanced, suggesting that "polymeric species" in **3c** has partly been transformed into dimeric species due to the hoist of temperature. Simultaneously, the free O–H stretching vibration absorption band intensity at 3580 $\mathrm{cm}^{-1}$ also increases in **3c** when the temperature changes from 20 to 60 °C. These indicate that polymeric species is the main existing pattern in **3c** and there is stronger hydrogen bond interaction in **3c** than in **3b**. This is consistent with the UV absorption spectra of **3a–c** and also further supports that the large nonlinear susceptibility in **3c** and **3b** has originated from the more regular arrangement of molecules induced by hydrogen bond interaction and increases with the increase in hydrogen bond interaction in molecules.

## 4. Conclusions

In conclusion, three novel organic nonlinear optical materials containing different hydroxyl group were synthesized and characterized. Their third-order nonlinear optical properties were investigated using Z-scan technique at 532 nm. Results reveal that the strong hydrogen bond interaction will induce molecular regular arrangement to result in larger $\chi^{(3)}$.

## Acknowledgements

This research was financially supported by the National Natural Science Fund of China (Grant no. 90206014 and 50472038) and the Outstanding Youth Fund of Anhui Province (Grant no. 04044060).

## References

[1] Bredas JL, Adant C, Tackx P, Persoons A. Chem Rev 1994;95:243.
[2] Rojo R, Yamada S, Matsuda H, Yankelevich D. Appl Phys Lett 1998;72:1021.
[3] Yesodha SK, Pillai CKS, Tsutsumi N. Prog Polym Sci 2004;29:45.
[4] Priyadarshy S, Therien MJ, Beratan DN. J Am Chem Soc 1996;118:1504.
[5] Torre G, Torres T, Lopez FA. Adv Mater 1997;9:265.
[6] Hu AT, Wang WY, Chen JR, Liu LC, Tai CH, Wei TH. Dyes Pigments 2004;62:11.
[7] Masse CE, Vanerwiede K, Kim WH, Jiang XL, Kumar J, Tripathy SK. Chem Mater 1995;7:904.
[8] Sukwattanasinitt M, Lee DC, Kim M, Wang XG, Li L, Yang K, et al. Macromolecules 1999;32:7361.
[9] Tang BZ, Xu HY. Macromolecules 1999;32:2569.
[10] Nomura R, Karim SMA, Kajii H, Hidayat R, Yoshino K, Masuda T. Macromolecules 2000;33:4313.
[11] Schuling A. Chem Phys Lett 1967;1:195.
[12] Rustagi KC, Ducuing J. Opt Commun 1974;10:258.
[13] Agrawal GP, Cojan C, Flytzanis C. Phys Rev B 1978;17:776.
[14] Prasad PN. SPIE 1986;682:120.
[15] Huggins KE, Son S, Stupp SI. Macromolecules 1997;30:5305.
[16] Li G, Song YL, Hou HW, Li LK, Fan YT, Zhu Y, et al. Inorg Chem 2003;42:913.
[17] Li L, Chen BY, Song YL, Li G, Hou HW, Fan YT, et al. Inorg Chim Acta 2003;344:95.
[18] Lu J, Lu CH, Yu JH, Xu JQ, Li Y, Zhang X, et al. Polyhedron 2004;23:755.
[19] Fan YT, Gang L, Li ZF, Hou HW, Mao H. J Mol Struct 2004;693:217.
[20] BaHae MS, Said AA, Wei TH, Hagan DJ, Stryland EWV. IEEE J Quantum Electron 1990;26:760.
[21] Ames DE, Bull D, Takundwa R. Synth Commun 1981;364.
[22] Haitjema HJ, Morgen GL, Tan YY, Challa G. Macromolecules 1994;27:6201.
[23] Wu YL, Demachi Y, Tsutsumi O, Kanazawa A, Shiono T, Ikeda T. Macromolecules 1998;31:4457.
[24] Wang J, Cao WF, Su JH, Tian H, Huang YH, Sun ZR. Dyes Pigments 2003;57:171.
[25] Xu XS, Ming H, Wang P, Liang ZC, Zhang QJ. J Opt A Pure Appl Opt 2002;4:L5.
[26] Liang Z, Ming H, Wang P, Zhang J, Xie J, Zhang QJ. J Appl Phys 2001;90:5866.
[27] Cesteros LC, Isasi JR, Katime I. Macromolecules 1993;26:7256.
[28] Xu HY, Kuo SW, Lee JS, Chang FC. Polymer 2002;43:5117.
[29] Finch JN, Lippincott ER. J Phys Chem 1957;61:894.
[30] Isasi JR, Cesteros LC, Katime I. Macromolecules 1994;27:2200.
[31] Xie JX, Chang JB, Wang XM, editors. The application of IR spectrum in organic and medical chemistry. Beijing: Scientific Press; 2001 [in Chinese].